Supplementary Information (SI) for Organic & Biomolecular Chemistry.
This journal is © The Royal Society of Chemistry 2025

Electronic Supporting Information

for

Antiadhesive glycoconjugate metal complexes targeting pathogens *Pseudomonas aeruginosa* and *Candida albicans*

Karolina Wojtczak,[a,b] Emilie Gillon,[c] Diana Bura,[d] Karen Richmond,[e] Megan Joyce,[e] Emma Caraher,[e] Keela Kessie,[f] Trinidad Velasco-Torrijos,[f] Cristina Trujillo,[g,d] Anne Imberty,[c] Kevin Kavanagh,[h] Gordon Cooke,[e] Joseph P. Byrne*[a,b,i,j]

[a.] *School of Biological and Chemical Sciences, University of Galway, University Road, Galway, Ireland.*
[b.] *UCD School of Chemistry, University College Dublin, Belfield, Dublin 4, Ireland.*
[c.] *Université Grenoble Alpes, CNRS, CERMAV, Grenoble 38000, France*
[d.] *School of Chemistry, Trinity Biomedical Sciences Institute, Trinity College Dublin, 152-160 Pearse St., Dublin 2, Ireland*
[e.] *School of Chemical and BioPharmaceutical Sciences, TU Dublin*
[f.] *Department of Chemistry, Maynooth University, Maynooth, Co. Kildare, Ireland*
[g.] *Department of Chemistry, The University of Manchester, Oxford Road, Manchester, M13 9PL, UK*
[h.] *Department of Biology, Maynooth University, Maynooth, Co. Kildare, Ireland*
[i.] *UCD Conway Institute for Biomedical and Biomolecular Research, Belfield, Dublin 4, Ireland.*
[j.] *UCD One Health Centre, University College Dublin, Belfield, Dublin 4, Ireland.*
* joseph.byrne@ucd.ie

Supplementary data supporting the information presented in the main text of the article, its figures and experimental section are provided in this document, including:

1. NMR spectra

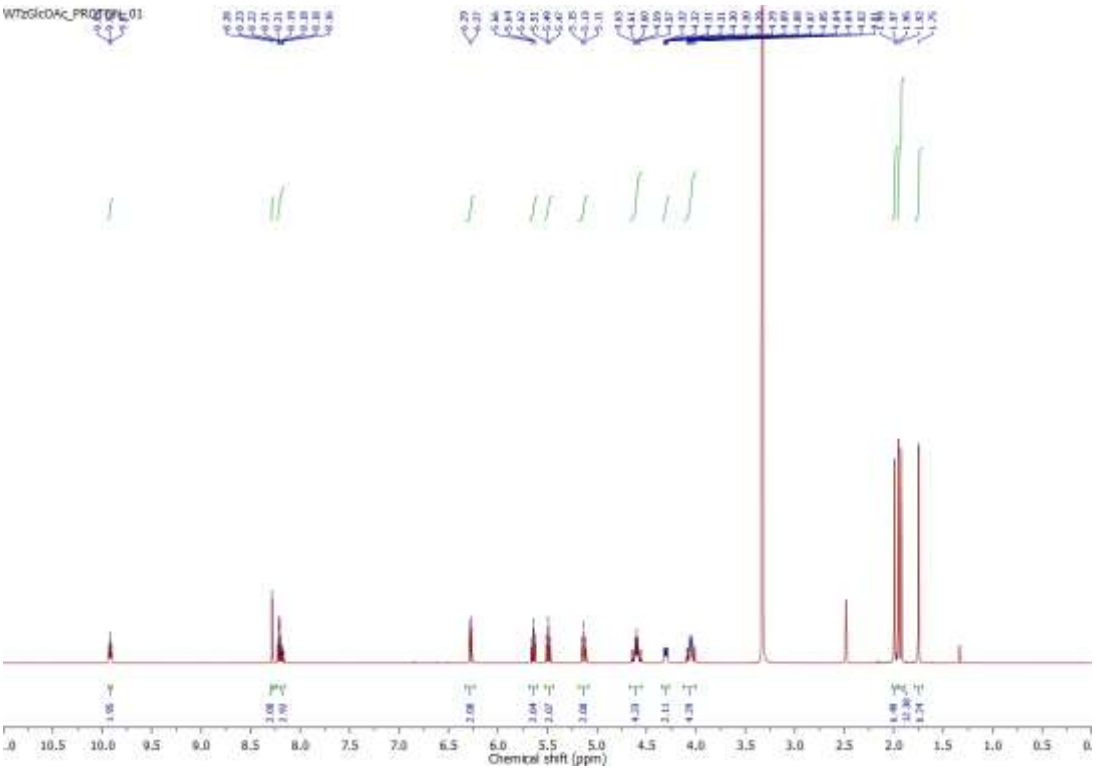

Figure S-1. *^{1}H NMR spectrum (500 MHz, DMSO-d_6) of* ***1Glc^{OAc}***

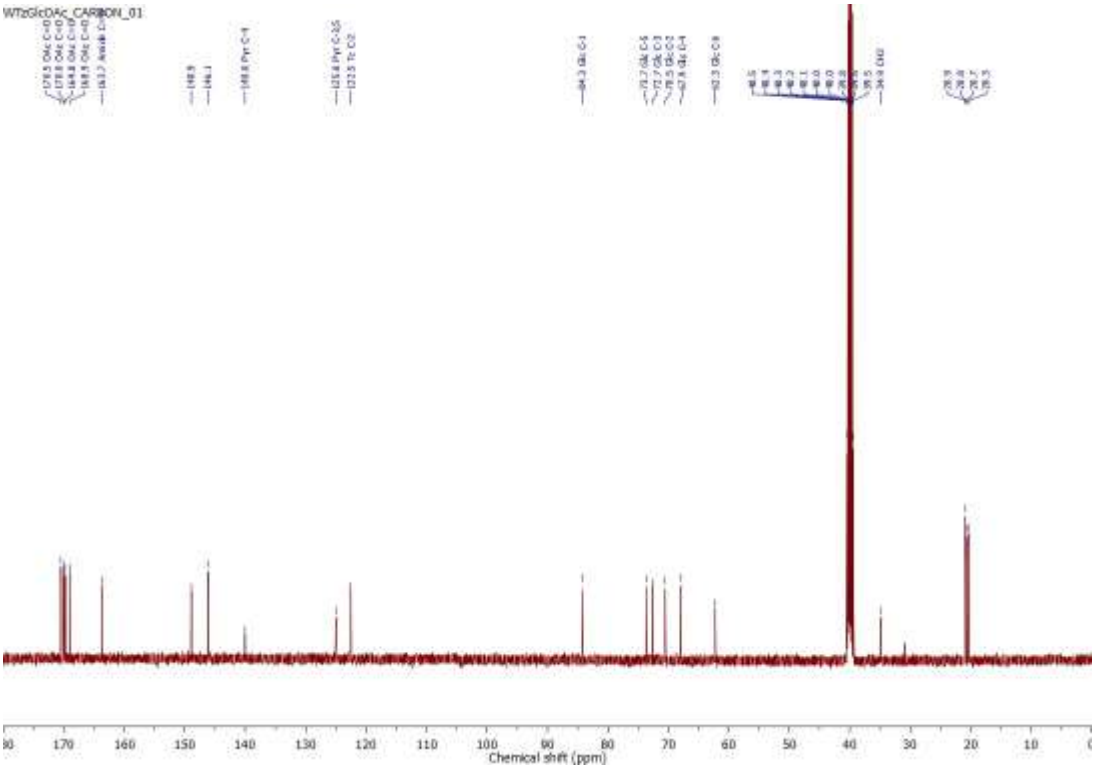

Figure S-2. *^{13}C NMR spectrum (126 MHz, DMSO-d_6) of* ***1Glc^{OAc}***

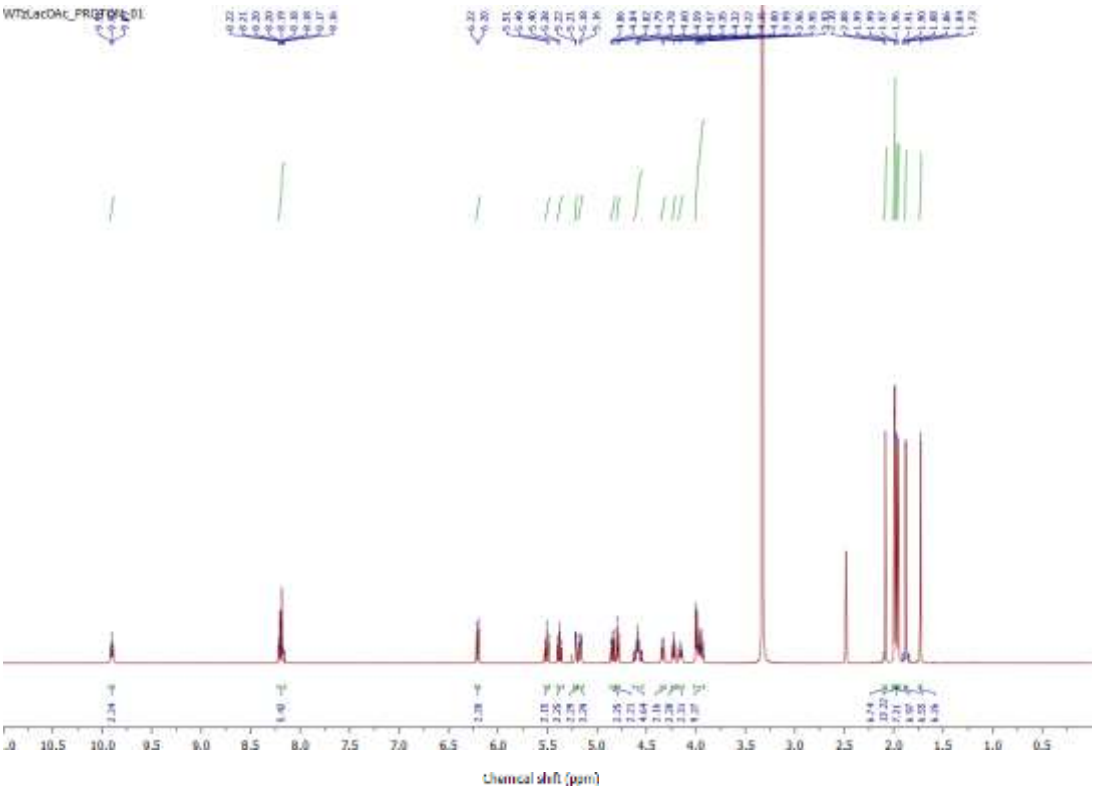

Figure S-3. *^{1}H NMR spectrum (500 MHz, DMSO-d_6) of* ***1Lac^{OAc}***

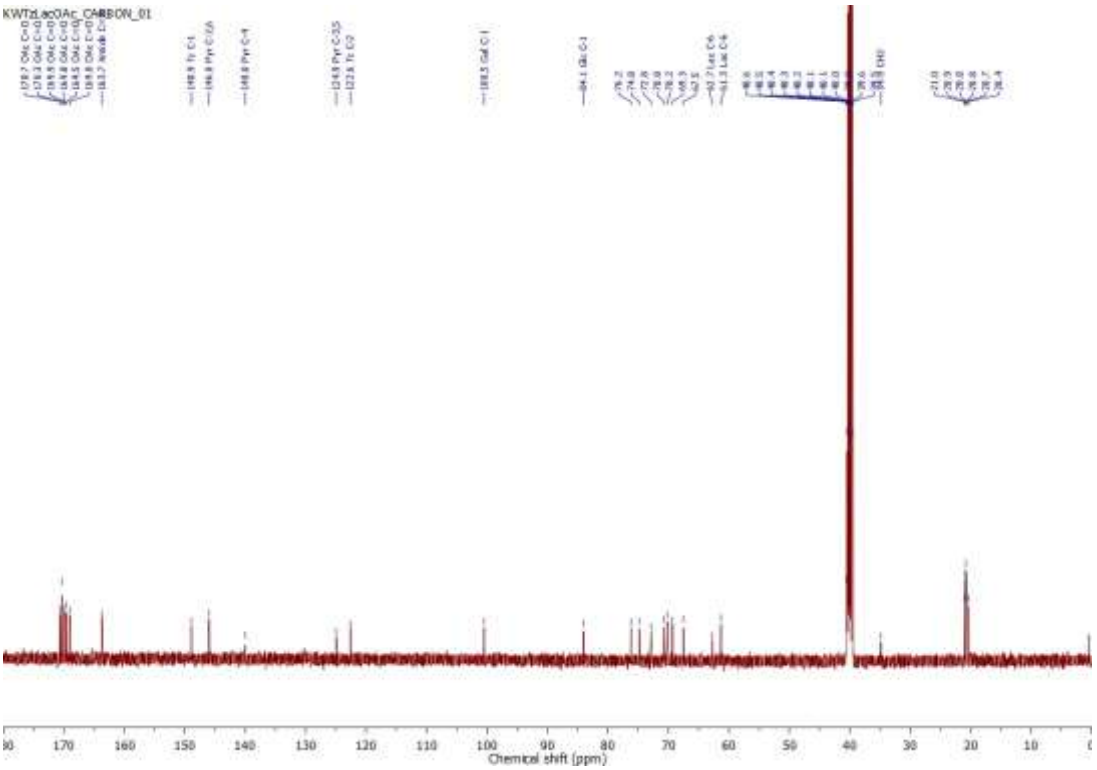

Figure S-4. *^{13}C NMR spectrum (126 MHz, DMSO-d_6) of* ***1Lac^{OAc}***

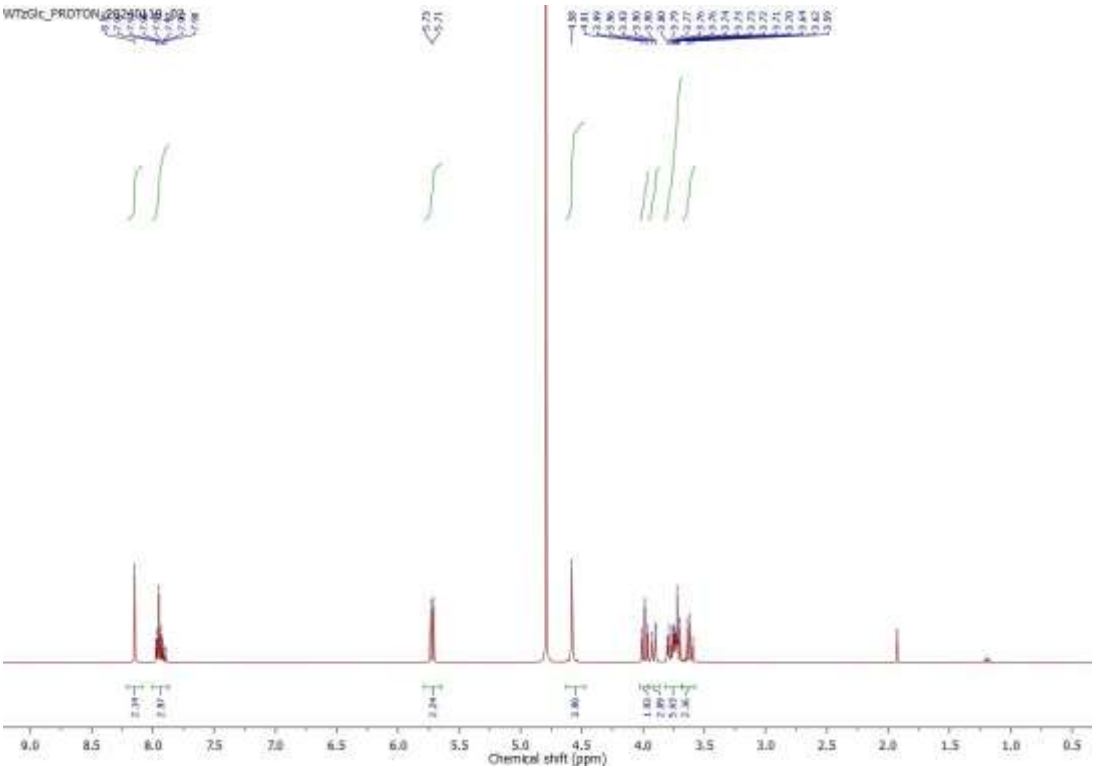

Figure S-5. *^{1}H NMR spectrum (400 MHz, D_2O) of* ***1Glc***

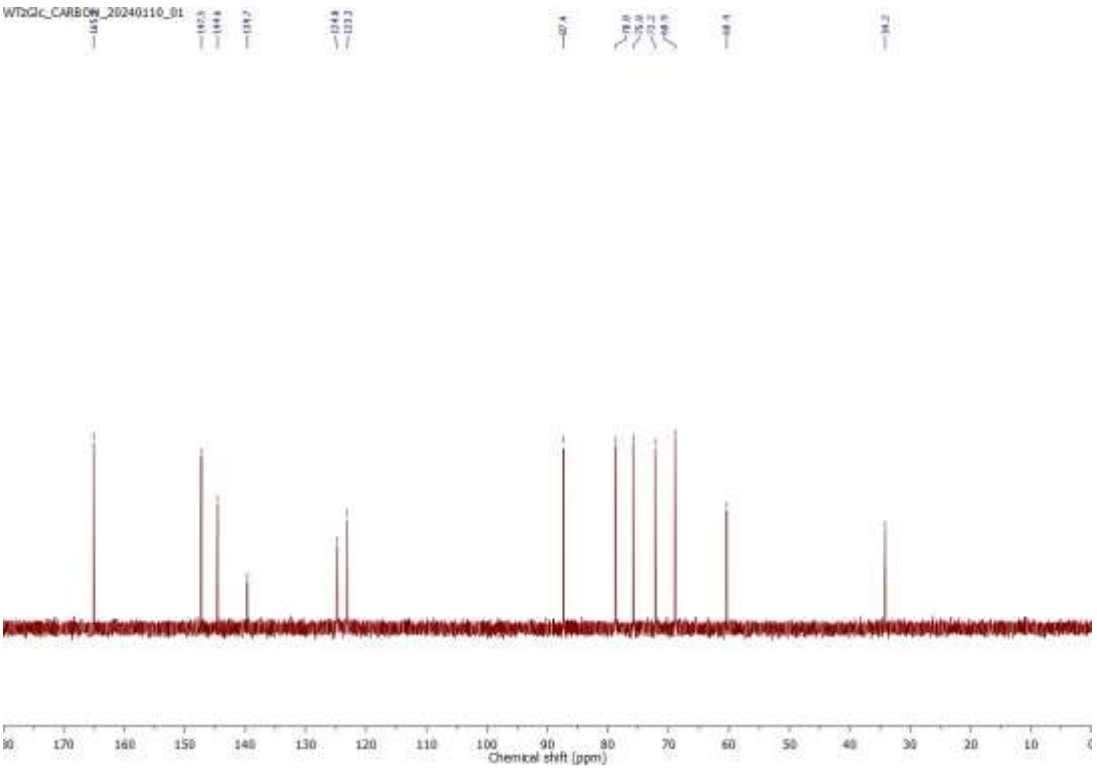

Figure S-6. *^{13}C NMR spectrum (101 MHz, D_2O) of* ***1Glc***

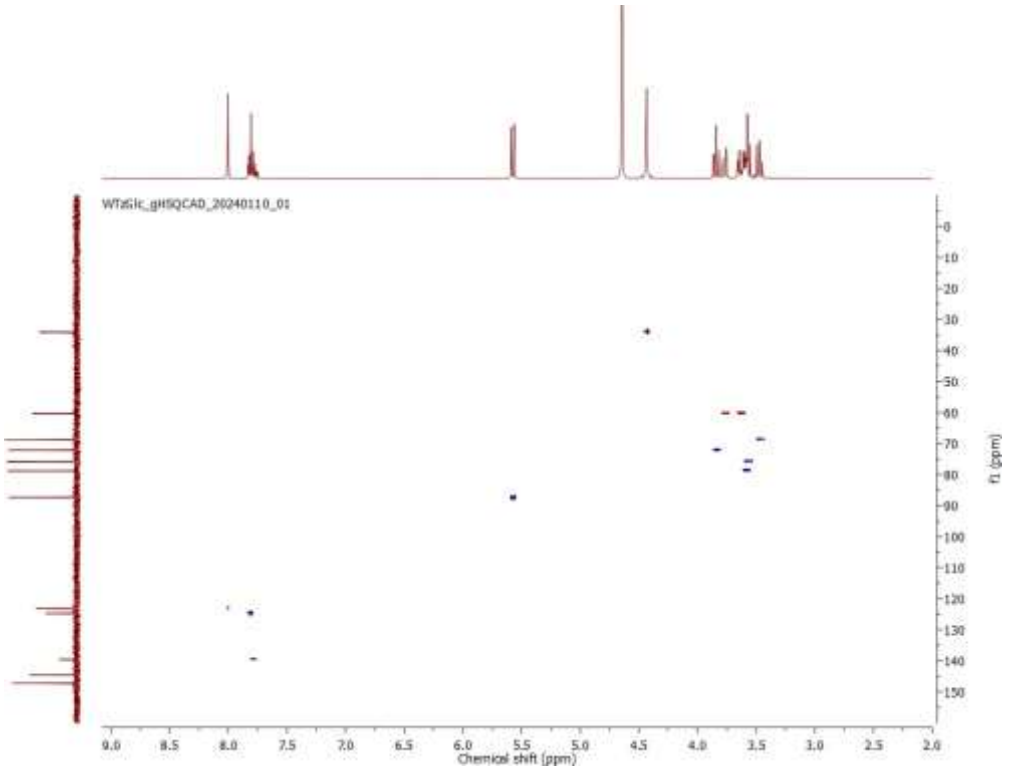

Figure S-7. *HSQC (D_2O) of* ***1Glc***

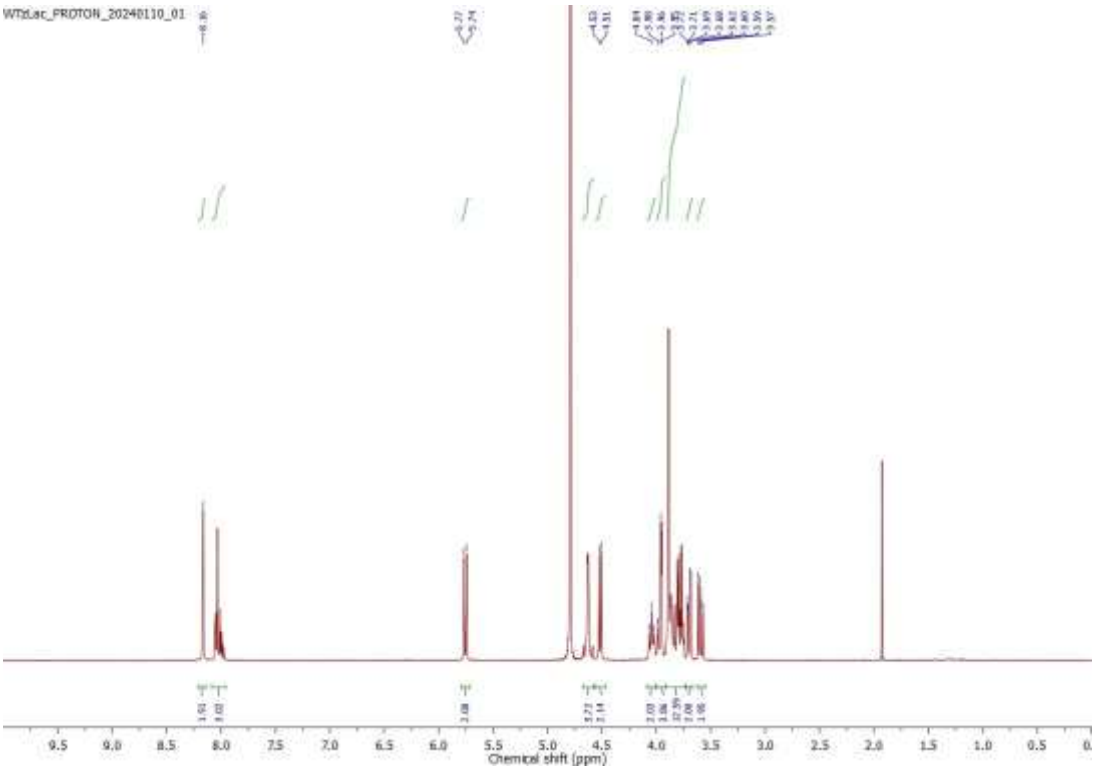

Figure S-8. *^1H NMR spectrum (400 MHz, D_2O) of* ***1Lac***

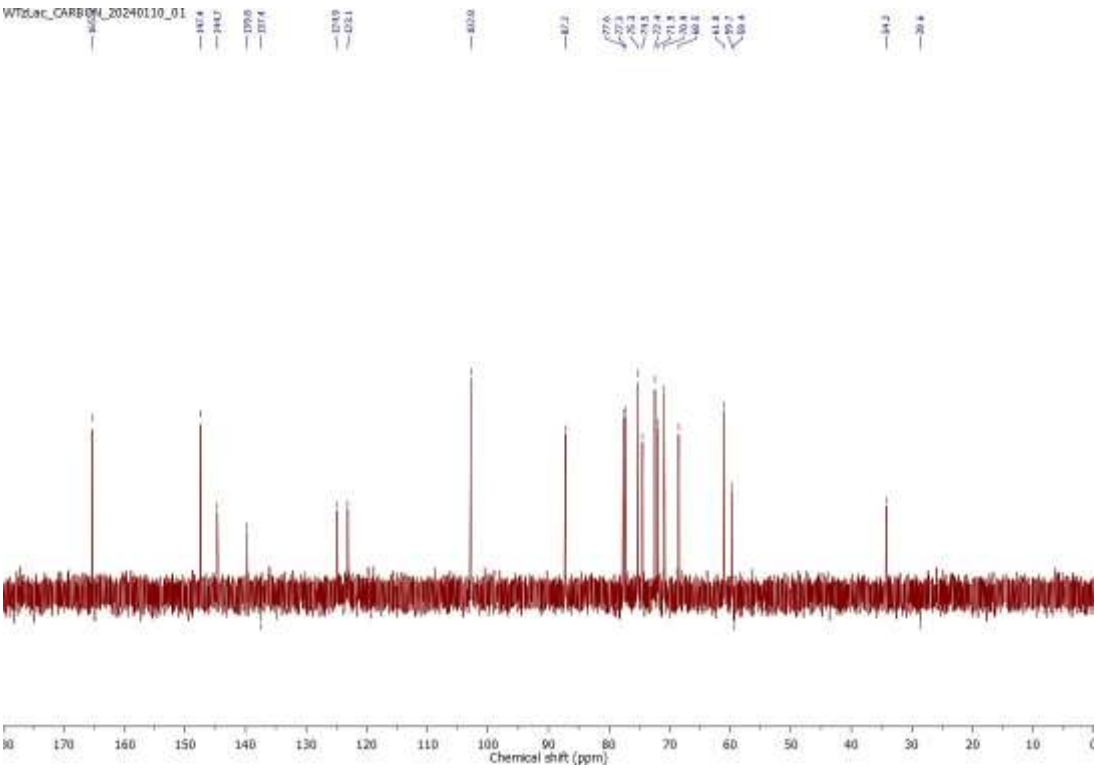

Figure S-9. *^{13}C NMR spectrum (101 MHz, D_2O) of* ***1Lac***

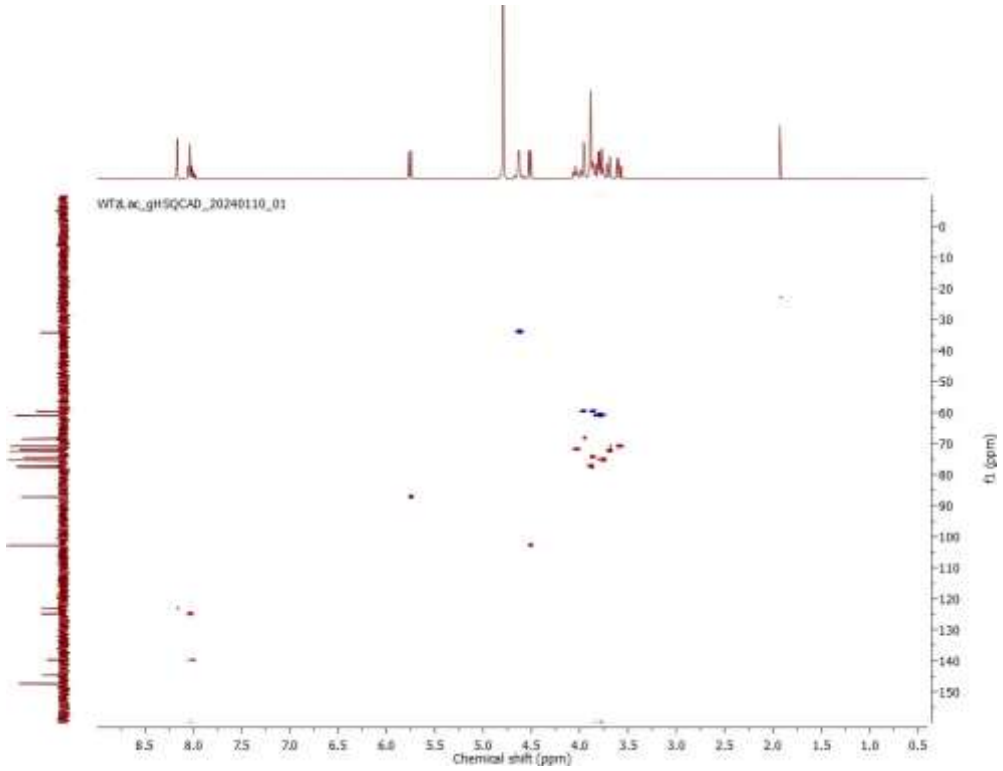

Figure S-10. *HSQC (D_2O) of* ***1Lac***

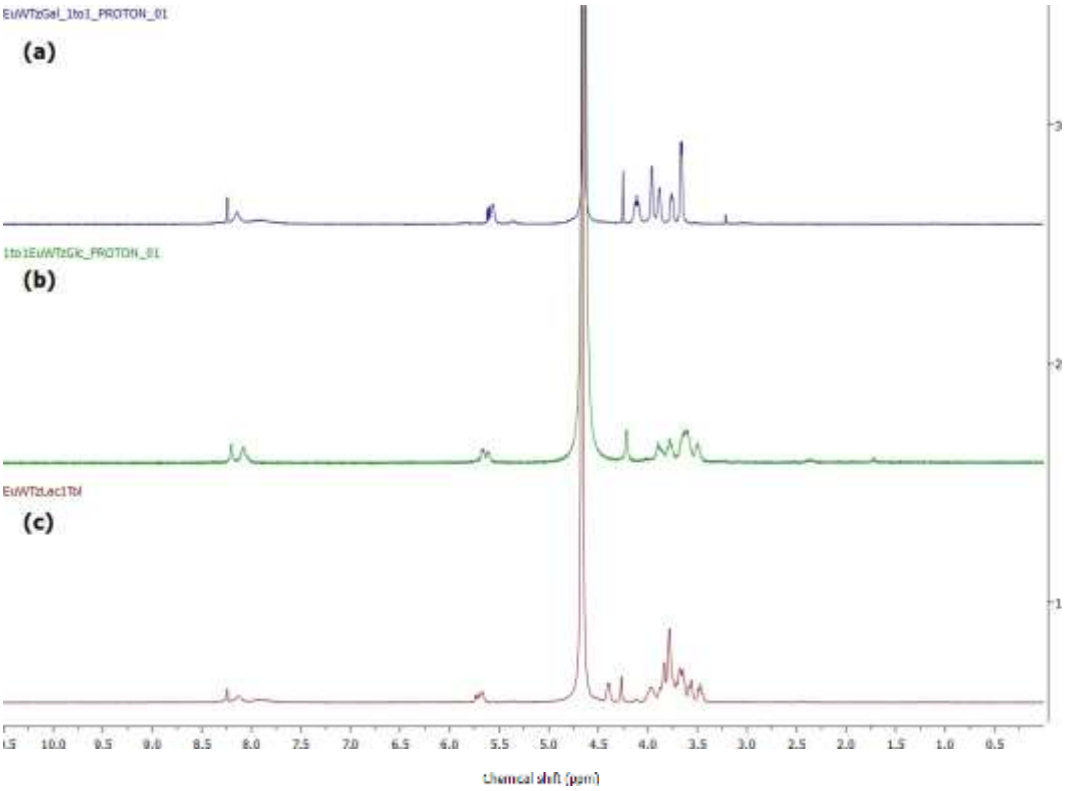

Figure S-11. *^{1}H NMR spectra (500 MHz, D_2O) of 1:1 Eu(III) complexes (a) [Eu(**1Gal**)]$(CF_3SO_3)_3$, (b) [Eu(**1Glc**)]$(CF_3SO_3)_3$, (c) [Eu(**1Lac**)]$(CF_3SO_3)_3$.*

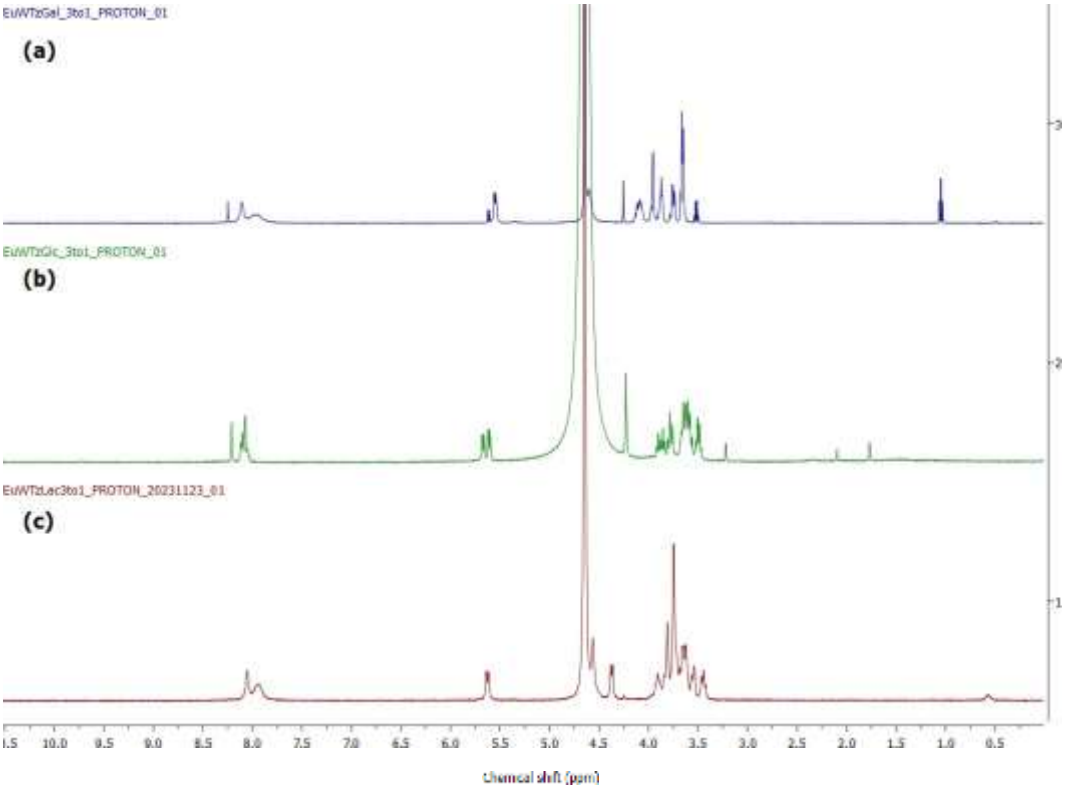

Figure S-12. *^{1}H NMR spectra (500 MHz, D_2O) of 1:3 Eu(III) complexes (a) [Eu(**1Gal**)$_3$]$(CF_3SO_3)_3$, (b) [Eu(**1Glc**)$_3$]$(CF_3SO_3)_3$, (c) [Eu(**1Lac**)$_3$]$(CF_3SO_3)_3$.*

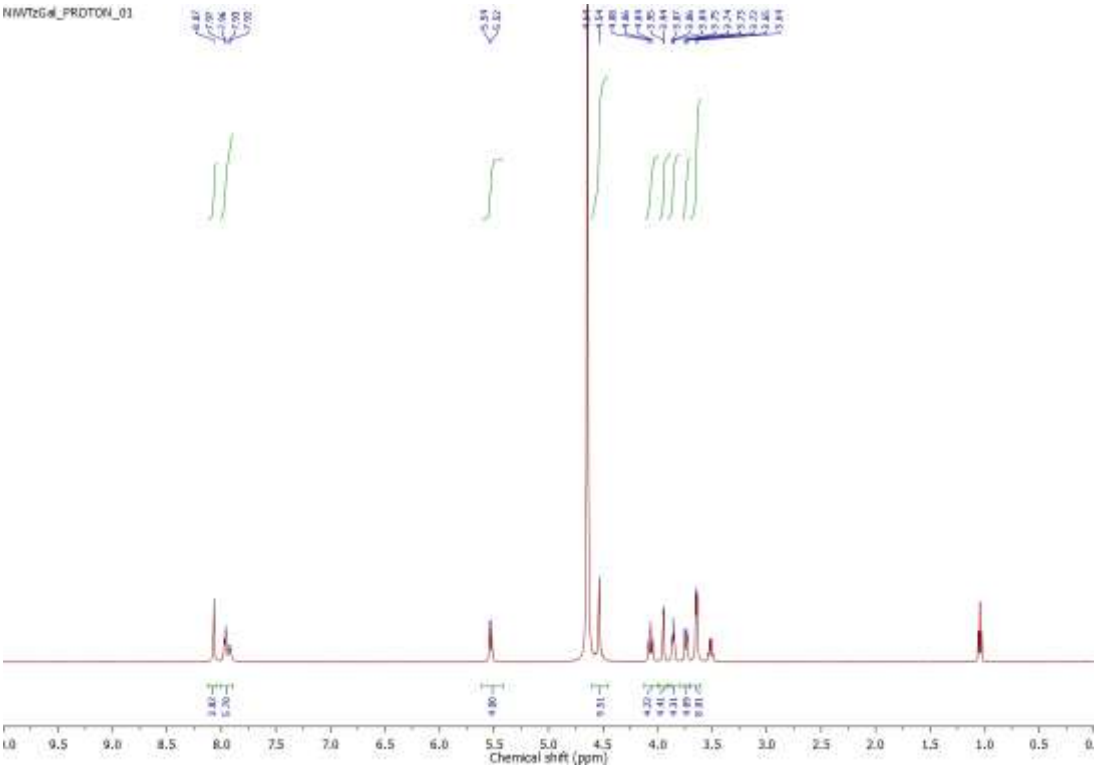

Figure S-13. *^{1}H NMR spectrum (500 MHz, D_2O) of [Ni(**1Gal**)$_2$]Cl$_2$*

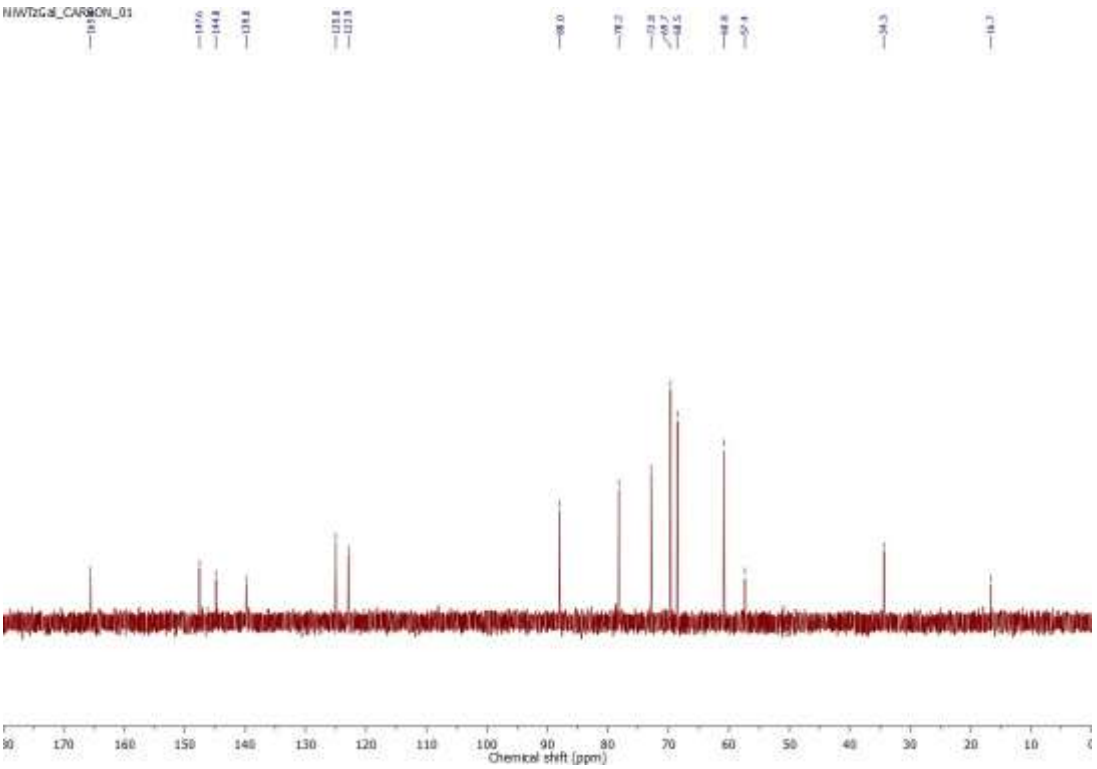

Figure S-14. *^{1}H NMR spectrum (126 MHz, D_2O) of [Ni(**1Gal**)$_2$]Cl$_2$*

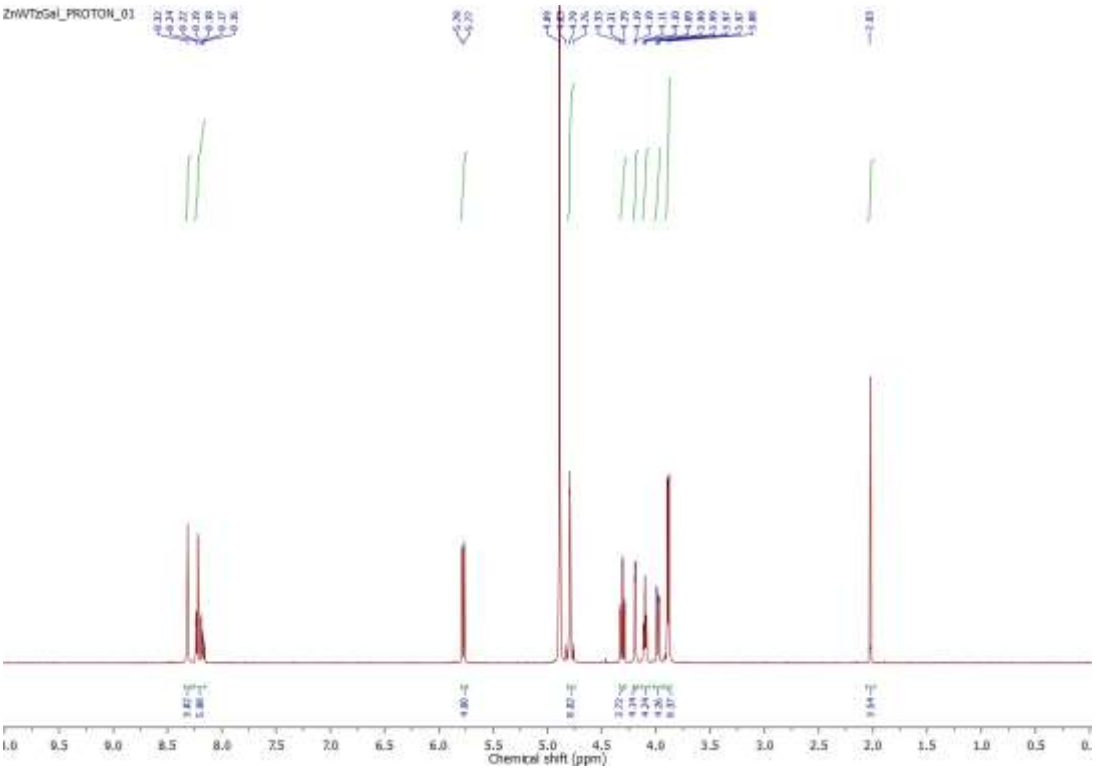

Figure S-15. *^{1}H NMR spectrum (500 MHz, D_2O) of [Zn(**1Gal**)$_2$](OAc)$_2$*

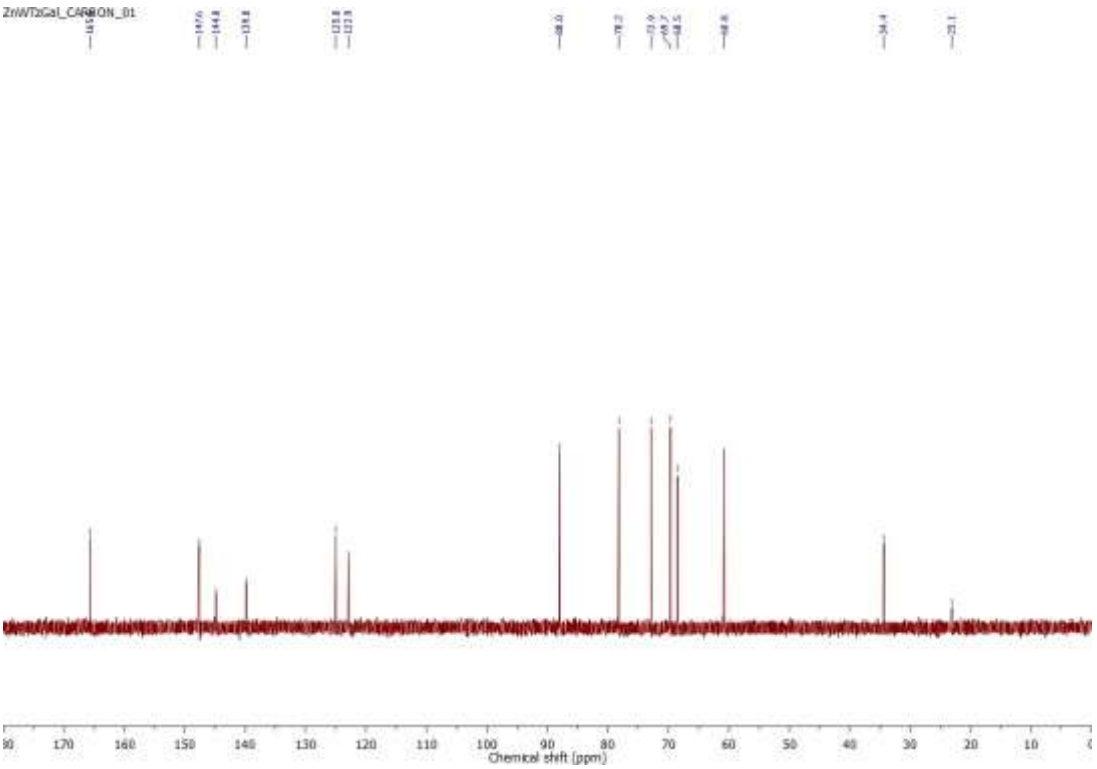

Figure S-16. *^{13}C NMR spectrum (126 MHz, D_2O) of [Zn(**1Gal**)$_2$](OAc)$_2$*

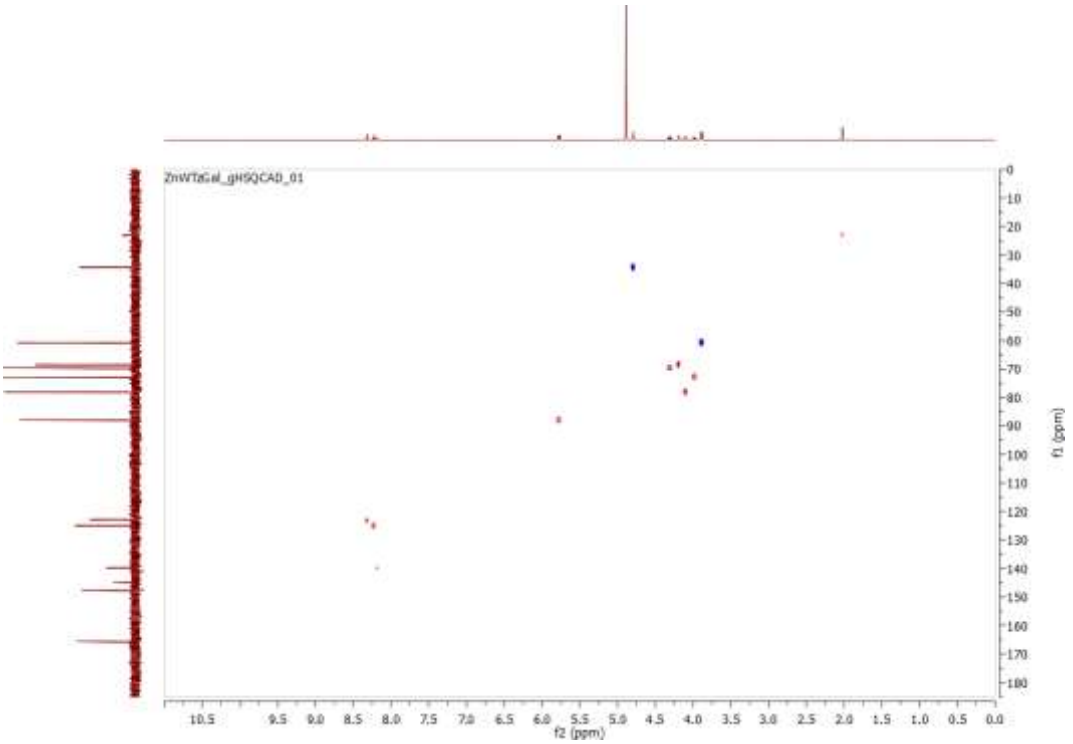

Figure S-17. *HSQC of [Zn(**1Gal**)$_2$](OAc)$_2$ in D_2O.*

2. Infrared spectra

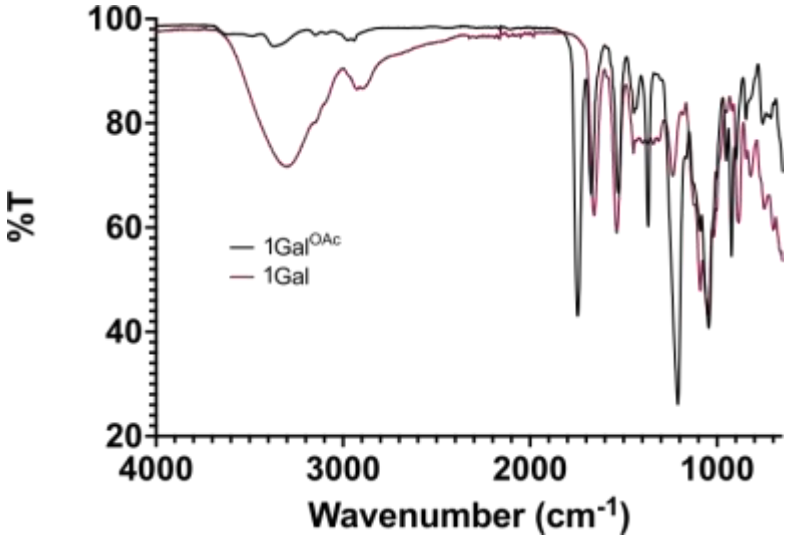

Figure S-18. *IR spectra of* ***1Gal***^{OAc} *and deprotected ligand* ***1Gal****.*

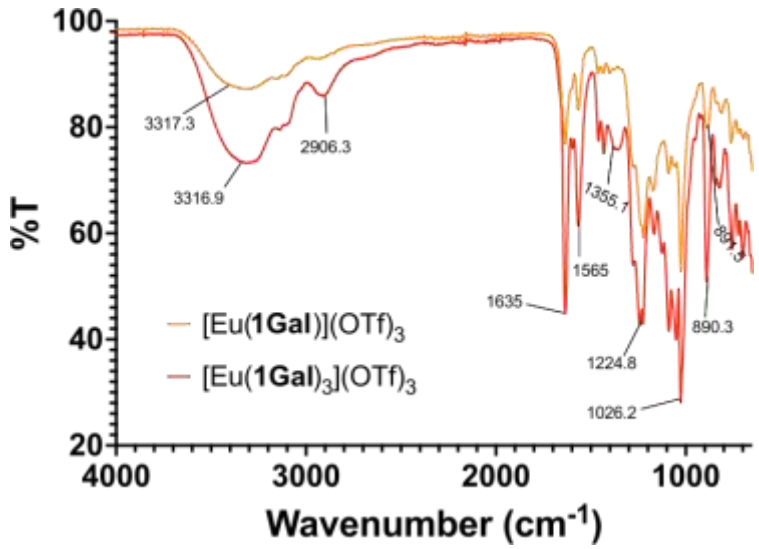

Figure S-19. *IR spectra of both Eu(III) complexes of* ***1Gal****.*

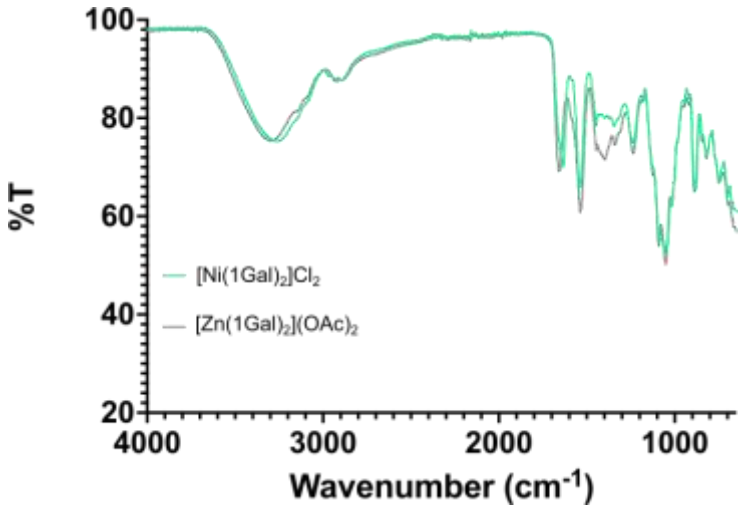

Figure S-20. *IR spectra of [Ni(****1Gal****)₂]Cl₂ and [Zn(****1Gal****)₂](OAc)₂*

3. ITC and SPR data

Isothermal calorimetry titration and fit data for compound **1Gal** is provided in Figure 2 of the main text of the article. Data for compound **5** (synthesis previously reported[S1]) is provided here.

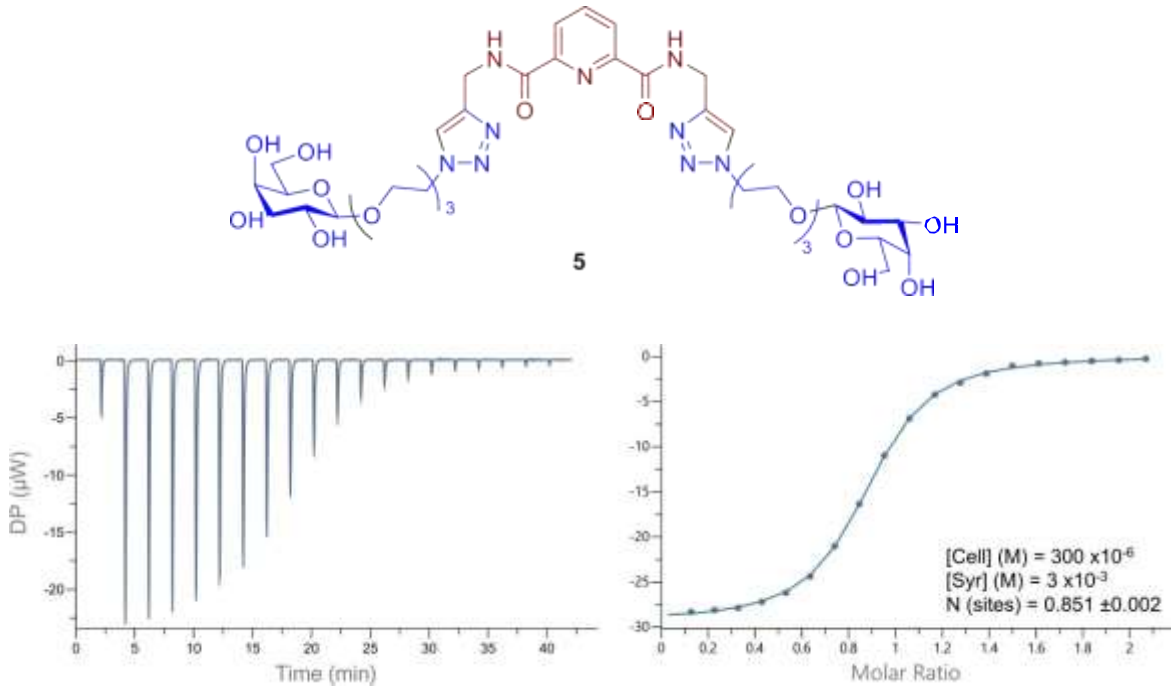

Figure S-21. *Structure of ligand **5**, and isothermal calorimetry titration and fitting in 10 mM Tris/HCl buffer (pH 7.2, 100 mM NaCl, 10 µM $CaCl_2$), [LecA] = 300 µM.*

Table S-1. *Thermodynamic properties calculated from ITC analysis for ligands **1Gal** and **5** binding to LecA in 10 mM Tris/HCl buffer (pH 7.2, 100 mM NaCl, 10 µM $CaCl_2$)*

Compound	K_d (µM)	**N**	**ΔH** (kJ mol^{-1})	**−TΔS** (kJ mol^{-1})	**ΔG** (kJ mol^{-1})
1Gal	9.6 ± 0.7	1	−29.0	+0.5	−28.5
5	6.5 ± 0.1	1	− 29.5	−0.2	−29.6

One replicate of surface plasmon resonance sensogram and fit for compound **1Gal** is provided in Figure 2 of the main text of the article. Data of duplicates for both **1Gal** and compound **5** (synthesis previously reported[S1]) is provided here.

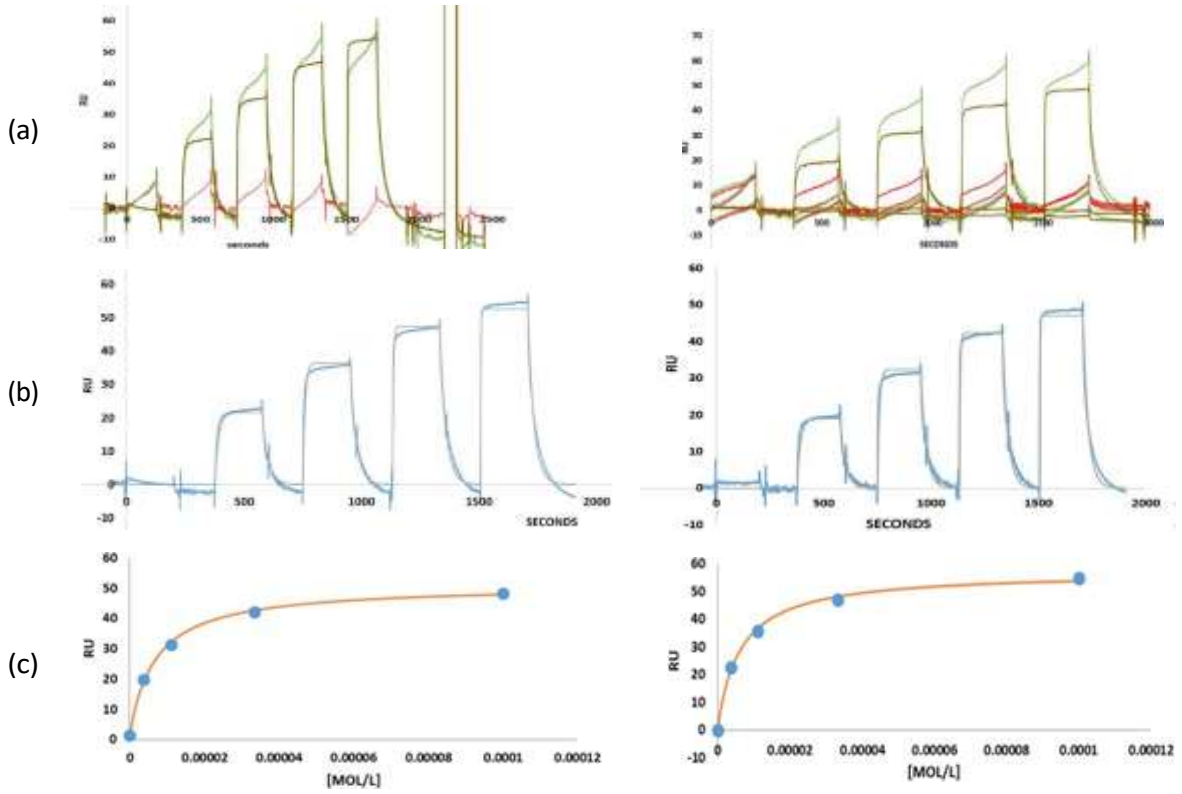

Figure S-22. *Surface plasmon resonance data (in duplicate) for compound **1Gal** with LecA-functionalised CM-5 chip, carried out in PBS buffer (10 mM phosphate buffer pH 7.4, 2.7 mM KCl, 137 mM NaCl, 100 µM $CaCl_2$, 0.05% Tween 20) with increasing concentration [**1Gal**] = 0 – 100 µM. (a) Sensograms, (b) kinetic fitting (fit in grey line), and (c) affinity fitting graphs.*

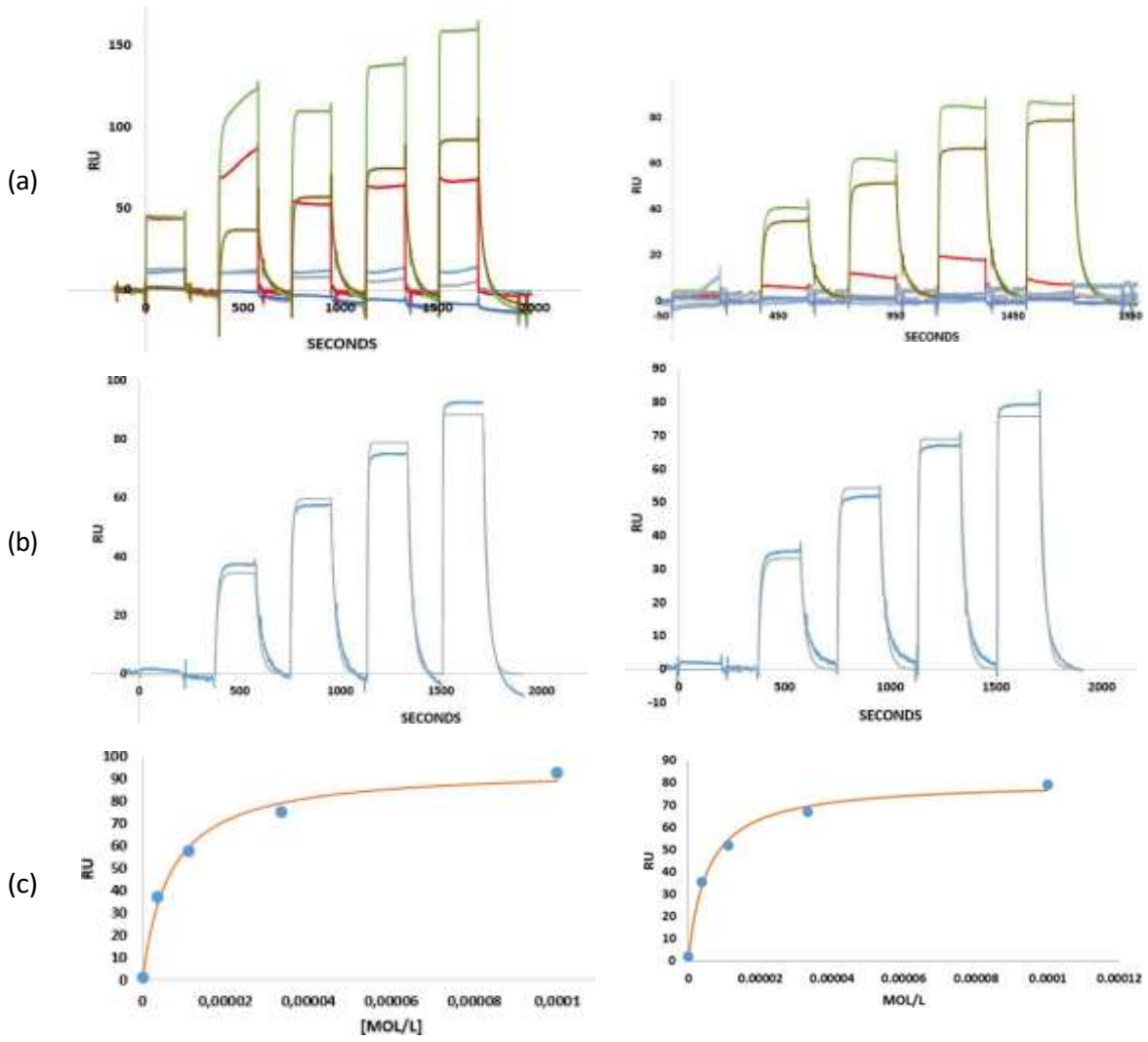

Figure S-23. *Surface plasmon resonance data (in duplicate) for compound **5** with LecA-functionalised CM-5 chip, carried out in PBS buffer (10 mM phosphate buffer pH 7.4, 2.7 mM KCl, 137 mM NaCl, 100 µM $CaCl_2$, 0.05% Tween 20) with increasing concentration [**5**] = 0 – 100 µM. (a) Sensograms, (b) kinetic fitting (fit in grey line), and (c) affinity fitting graphs.*

Table S-2. *Data from SPR measurements of compounds **1Gal** and **5**. Values are average of duplicates. K_d values for both kinetic and steady state model are given.*

Compound	k_{on} (1/Ms)	k_{off} (1/s)	K_d (µM)	R_t (min)	Steady state K_d (µM)
1Gal	6643 ± 83	0.0394 ± 0.0004	5.9 ± 0.1	0.4	6.6 ± 0.5
5	7499 ± 935	0.043 ± 0.001	5.8 ± 0.9	0.4	6.0 ± 1.0

4. UV/Vis and Emission spectra

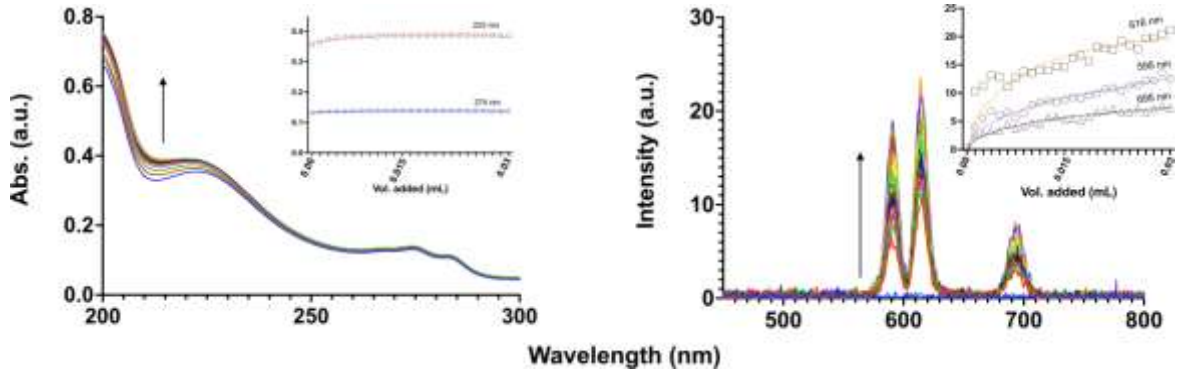

Figure S-24. *Self-assembly titration of an aqueous solution of* ***1Gal*** *(working concentration = 2 × 10^{-5} M) upon successive addition of aliquots of $Eu(CF_3SO_3)_3$ (stock solution concentration 1.1 × 10^{-3} M). Left: Changes in UV-Vis absorbance spectra; Right: changes in phosphorescence spectra. Insets show binding isotherms at selected wavelengths (points) and calculated fits (lines).*

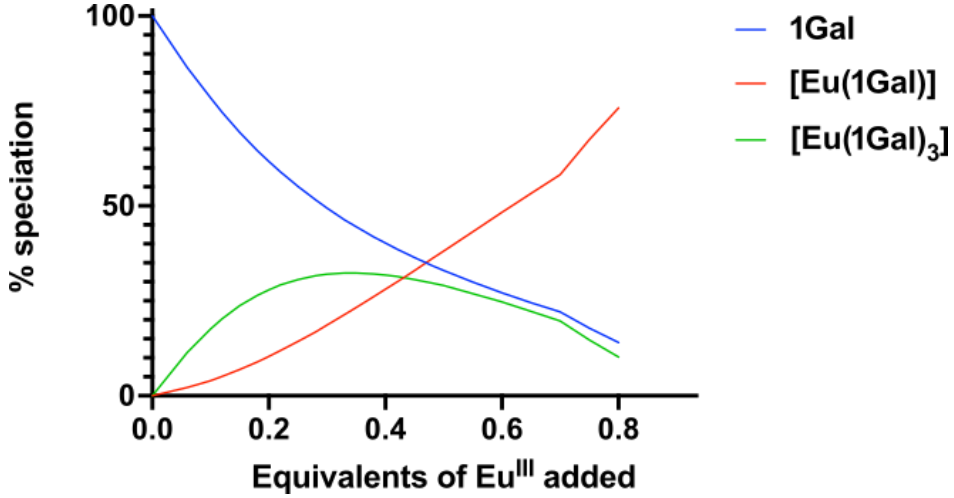

Figure S-25. *Calculated speciation distribution diagram for UV-Vis absorption titration data in the figure above, as a function of [Eu^{3+}], the various traces showing the calculated distribution of ligand, 1:1 complex and 3:1 complex at various concentrations when fit using ReactLab Equilibrium (Jplus Consulting Pty Ltd).*

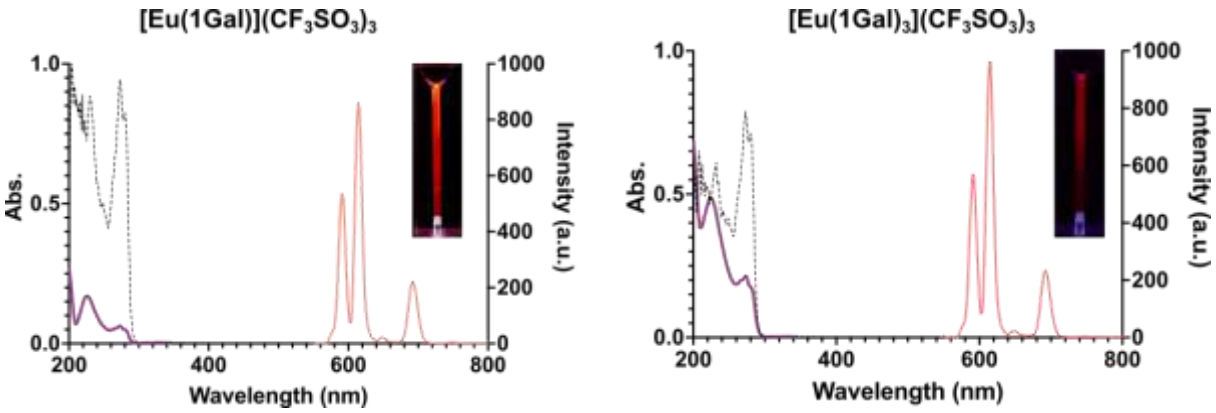

Figure S-26. *Photophysical characterisation of isolated Eu(III) complexes of* ***1Gal****. UV-vis absorbance spectra (purple line), phosphorescence emission spectra upon excitation at λ = 274 nm (red line), excitation spectra for λ_{em} = 614 nm (black dashed line). Insets: photographs of cuvettes containing these solutions under UV irradiation.*

5. Biological assay data with *P. aeruginosa*

Antimicrobial assays

Antimicrobial assays were carried out as described in the article's Experimental Section. Selected data was presented in Figure 4. Inhibition of bacterial growth by **1Gal**, each of its complexes and precursor metal salts (at various concentrations) is shown here – in most cases there was no inhibitory effect.

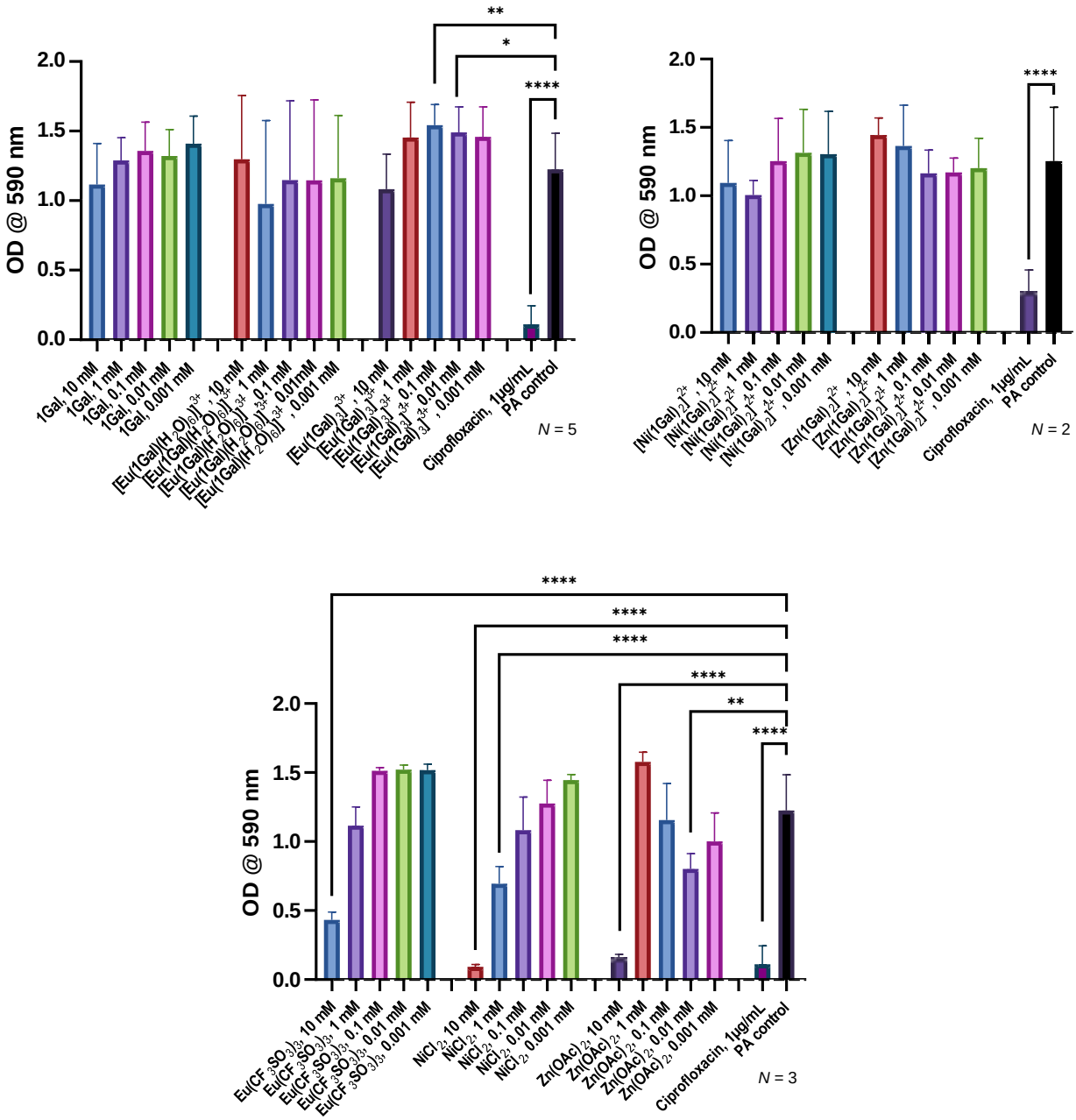

Figure S-27. *Full data from assays for bactericidal effects of ligand* ***1Gal*** *and its complexes against P. aeruginosa PAO1 strain at a range of concentrations.*

Anti-biofilm assays

Anti-biofilm assays were performed as described in the article's Experimental Section. Selected data was presented in Figure 4. Inhibition of bacterial growth by **1Gal** and each complex at various concentrations is shown here – only Eu(III) complexes showed significant inhibitory effects.

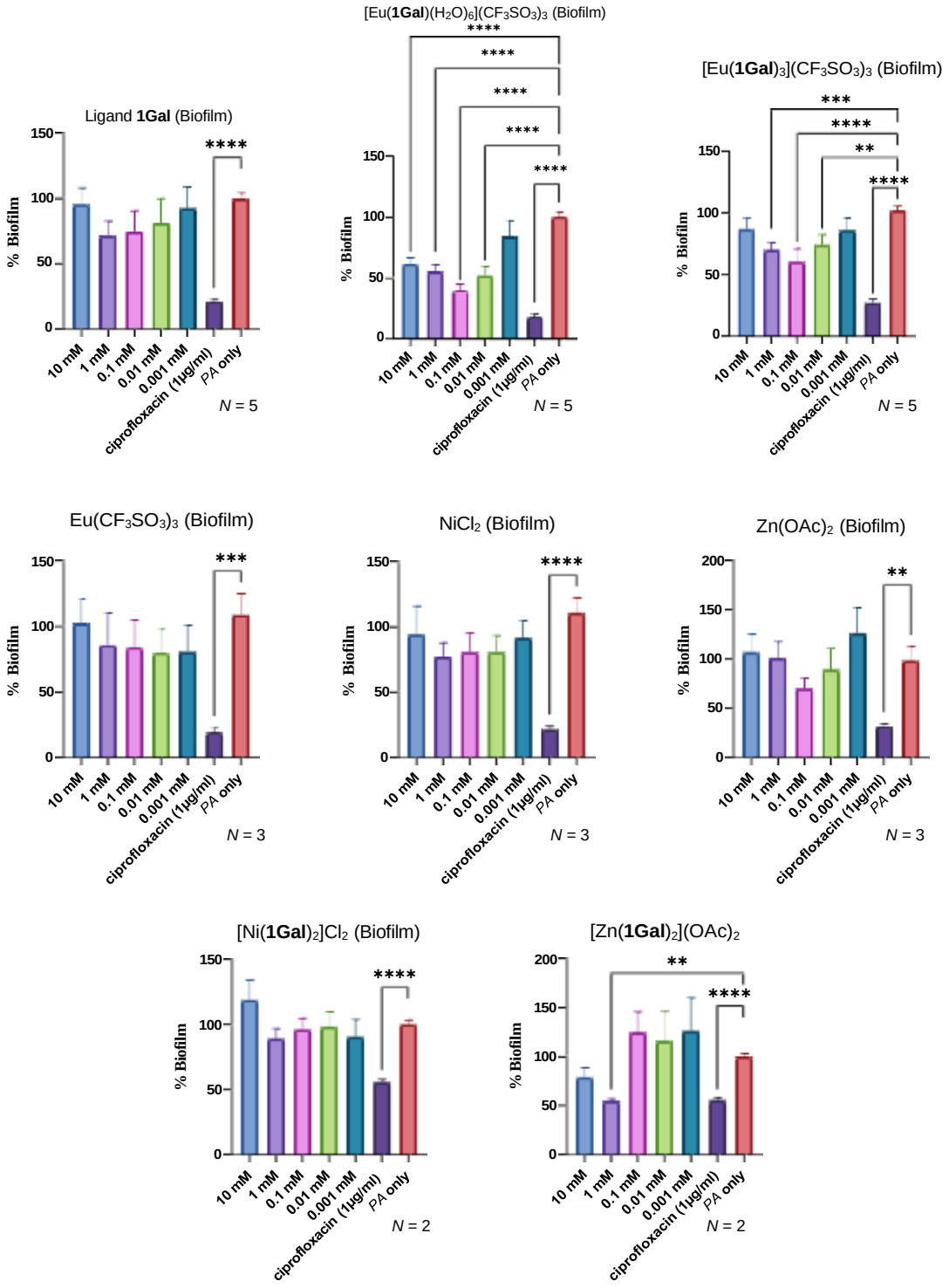

Figure S-28. *Full data from crystal violet assay for biofilm inhibition effects of ligand **1Gal**, its complexes, and precursor metal salts against P. aeruginosa PAO1 strain at a range of concentrations.*

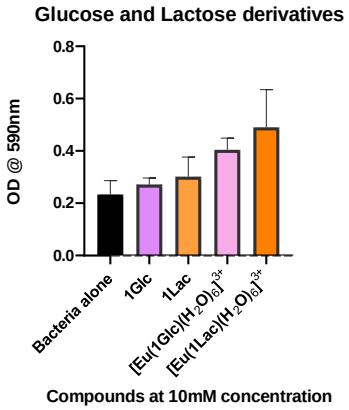

Figure S-29. *Data from crystal violet assay for biofilm inhibition effects of control ligands* ***1Glc*** *and* ***1Lac*** *(Scheme 1) and their 1:1 Eu(III) complexes against P. aeruginosa PAO1 strain at 10 mM. Inhibition observed for galactoside not replicated with other carbohydrate epitopes.*

6. DFT Calculations

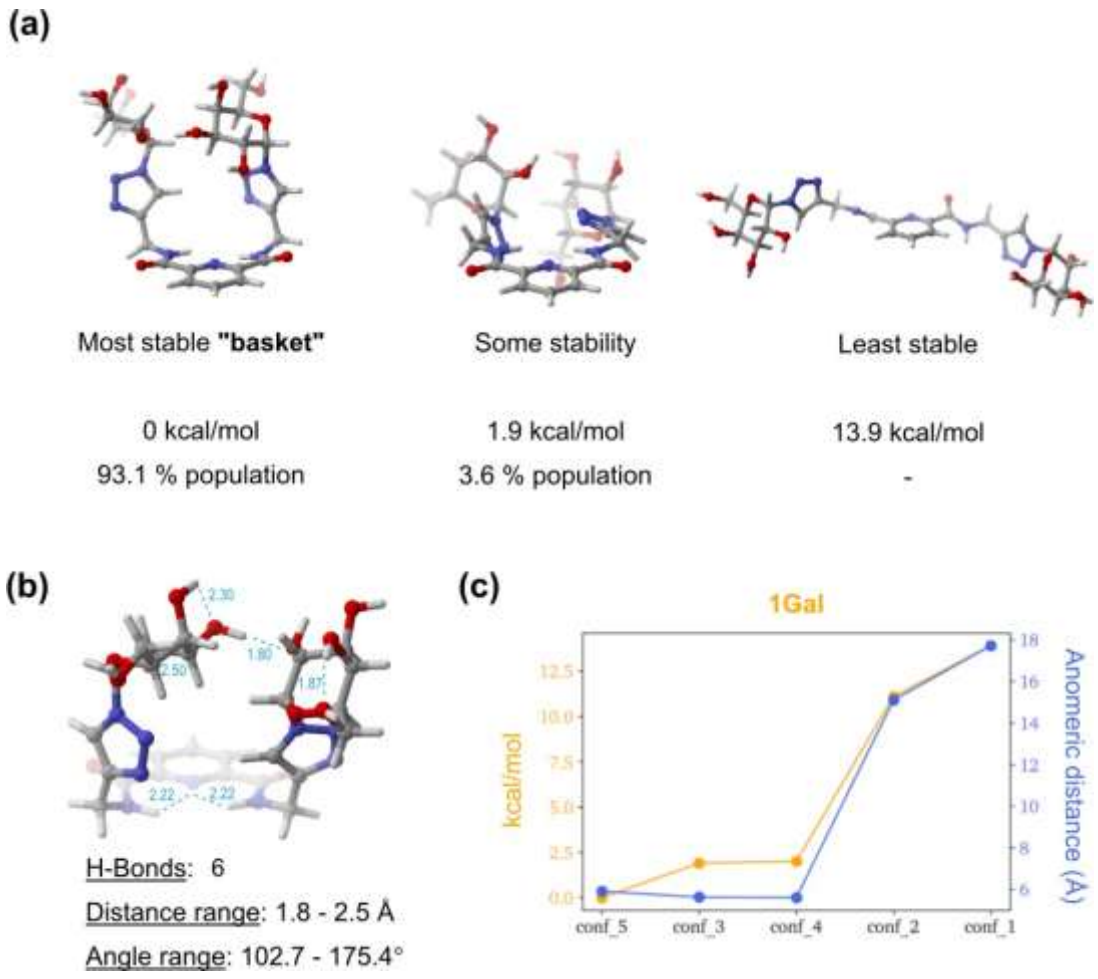

Figure S-30. *Conformational analysis of* ***1Gal*** *calculated by DFT. (a) Structures, relative energies and Boltzmann population of lowest energy, second lowest energy and highest energy conformers studied; (b) Hydrogen bonds (HBs) formed in the most stable conformer of* ***1Gal*** *and the variation in distances and angles of the HBs in all studied conformers; (c) Relative energies when compared to the most stable conformer (yellow) versus the distance between the anomeric carbons of the galactoside branches (blue).*

Table S-3. *Charge and multiplicity parameters used in conformational analysis of structures of* ***1Gal*** *and its complexes, as well as determined hydrogen bonds, distances and angles for each of the most stable conformers, and calculated distances between the anomeric carbons of the galactose units within each ligand.*

	Ligand 1Gal	$[Eu(1Gal)(H_2O)_6]^{3+}$	$[Ni(1Gal)_2]^{2+}$	$[Zn(1Gal)_2]^{2+}$
Charge	0	3+	2+	2+
Multiplicity	1	7	3	1
H-bonds	6	3	4	5
Distance range	1.80–2.50 Å	1.85–2.65 Å	1.77–2.07 Å	1.80–2.43 Å
Angle range	102.7– 175.4°	117.5– 150.1°	173.8–177.3°	128.7– 179.7°
Distance between anomeric C	5.90 Å	6.14 Å	7.04 Å , 7.04 Å	6.94 Å , 6.92 Å

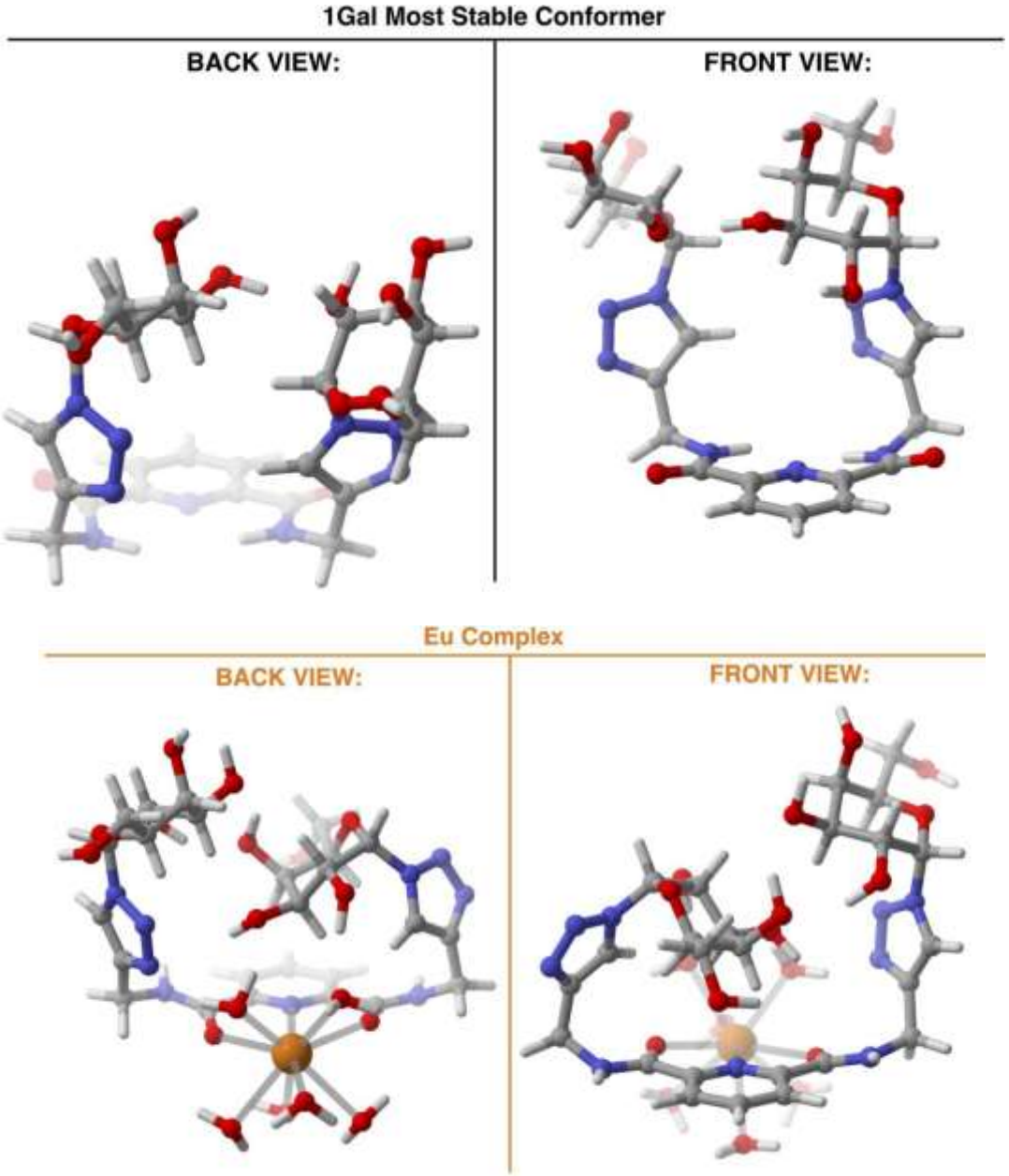

Figure S-31. *Structures of lowest energy conformers of* ***1Gal*** *and its Eu(III) complex, showed from front and back.*

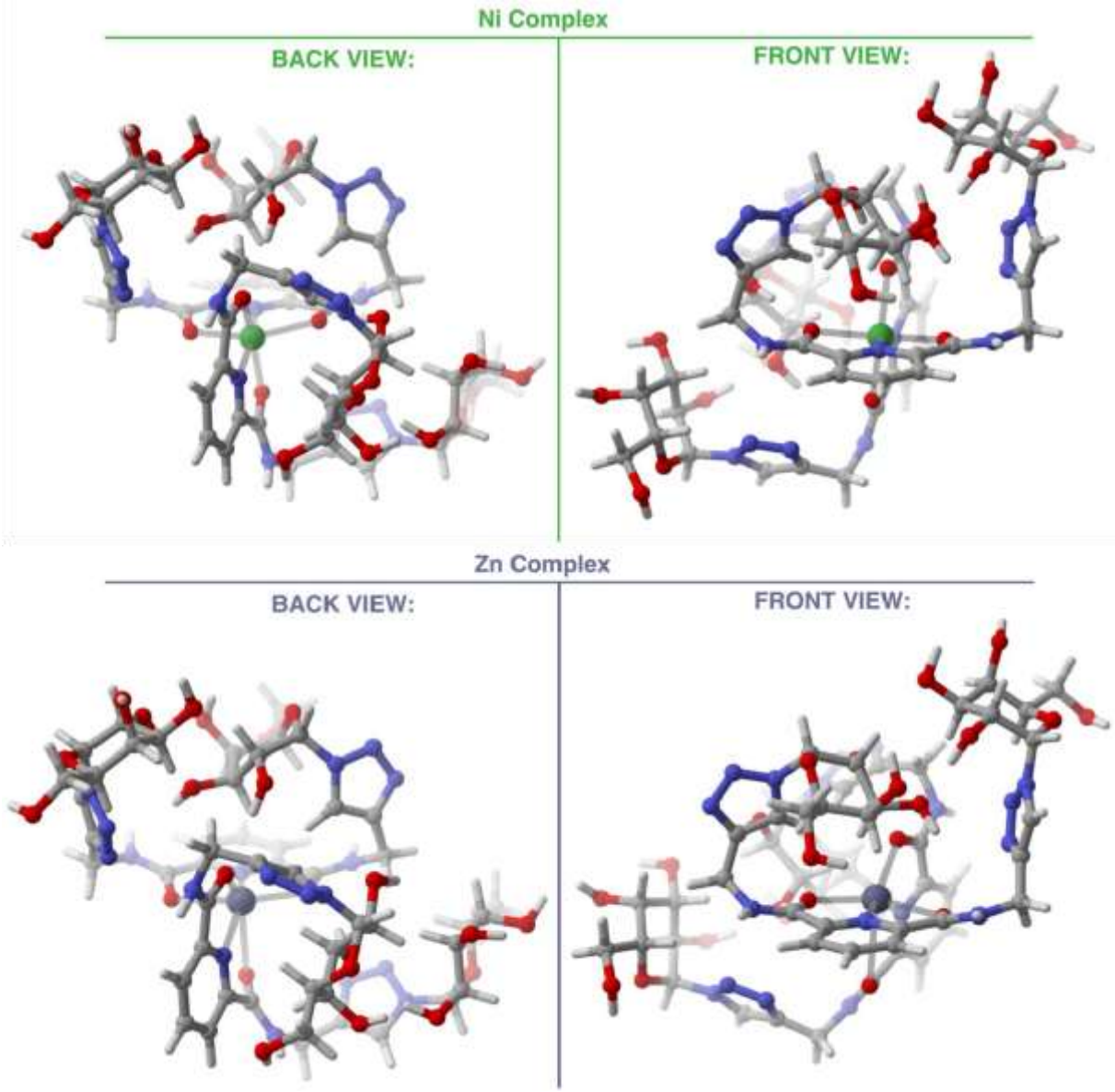

Figure S-32. *Structures of lowest energy conformers of Ni(II) and Zn(II) complexes, showed from front and back.*

7. Biological assay data with *C. albicans*

Toxicity assays with *C. albicans*

Toxicity to CA was assessed as follows: Saboraud-dextrose broth (Oxoid CM147) was prepared and sterilised along with all needed instrumentation by autoclave. Four sterile 96 well plates were placed in a laminar flow biological hood, and to each well was added 100 µL of the medium. To column 3 was added 100 µL of each compound tested in quadruplicate at a working concentration of 0.25 mM; this was then serially diluted up to column 11 with a final concentration of 0.001 mM. The original stock of CA culture was diluted by a factor of 1/200 by inoculating 200 µL into 40 mL of broth. The dilute culture was then added to each well in 100 µL aliquots for a total volume of 200 µL in each well. The plates were incubated at 37 °C for 24h and then their optical density was measured by a plate reader at 600 nm for each well. The data

contains an internal control for each replicate and each sample, and is reported as the % growth for each concentration with respect to this internal control.

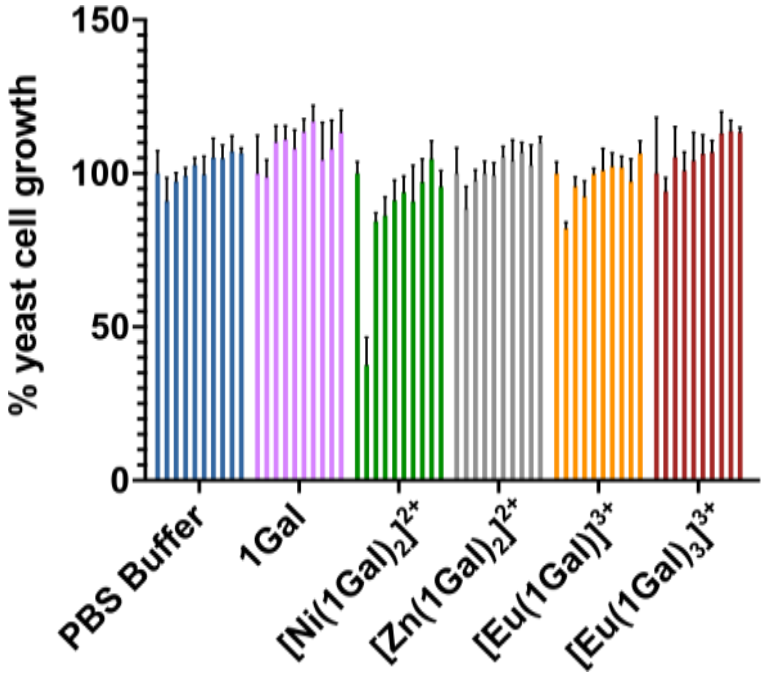

Figure S-33. *Results of toxicity assays C. albicans cells treated with various concentrations of* ***1Gal*** *and its complexes, compared to a control treated with the same volumes of PBS buffer. Each cluster of bars in the chart represent a serial dilution of concentrations of the glycoconjugate as follows (left–right): 0 mM, 0.250 mM, 0.125 mM, 0.063 mM, 0.031 mM, 0.016 mM, 0.008 mM, 0.004 mM, 0.002 mM, 0.001 mM.*

Control experiments for metal salt precursors with *C. albicans*

To ascertain whether or not metal salt precursors alone led to significant antiadhesive activity, $Eu(CF_3SO_3)_3$, $NiCl_2$ and $Zn(OAc)_2$ were tested under both pre-treatment exclusion assays and competition assays, in parallel with ligands **1Gal** and **3** as positive controls.

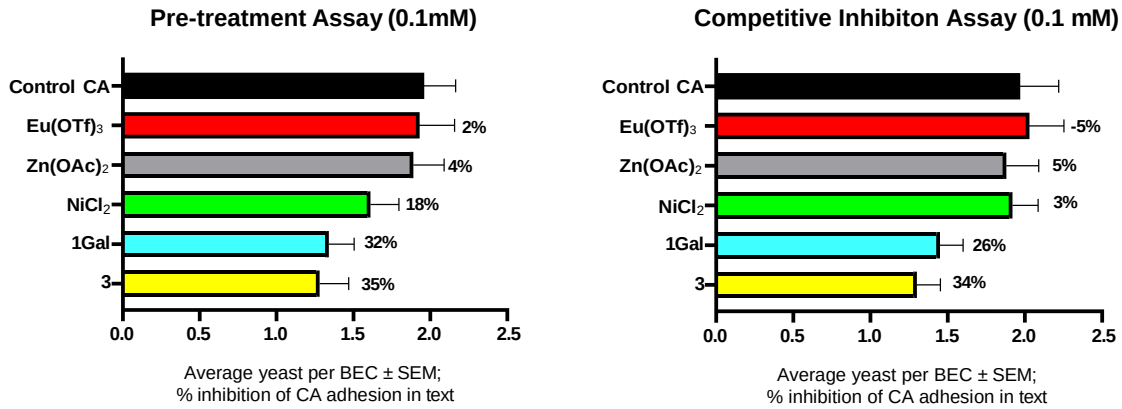

Figure S-34. *Average yeast cell count per BEC after pre-treatment and competitive assays with 0.1 mM concentrations of metal salt precursors, as well as compounds* ***1Gal****, and* ***3****, measured at the same time.*

Displacement assays of with glycoconjugate ligands

Adherence assays were based on methodology from previously published work and are reiterated in brief in the main text of the article.[S2] Data for pre-treatment exclusion assay and competition assay is presented in Figure 6 of the article, and described in the experimental section. In displacement assays, adherence was allowed to occur by mixing *C. albicans* cells and BECs in the absence of the glycoconjugate compound and allowing adherence to occur. The BEC/yeast cell mixture was harvested and re-incubated with the compound (**3** or **1Gal**, 1 mg/mL) for a further 90 minutes, after which time adherence is measured as in the other assay methodologies.

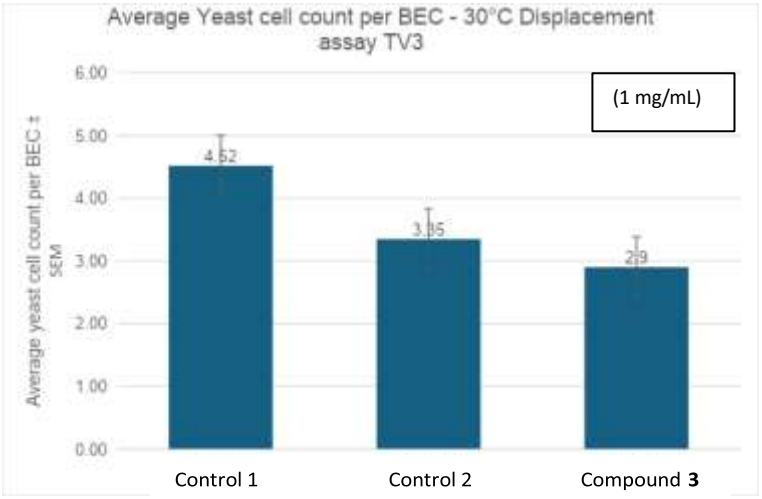

35.8 % reduction against control 1
and 13.4 % reduction against control 2

Figure S-35. *Average yeast cell count per BEC after a displacement assay with compound* ***3****,*[S2] *at a concentration of 1 mg/mL (1.5 mM)*

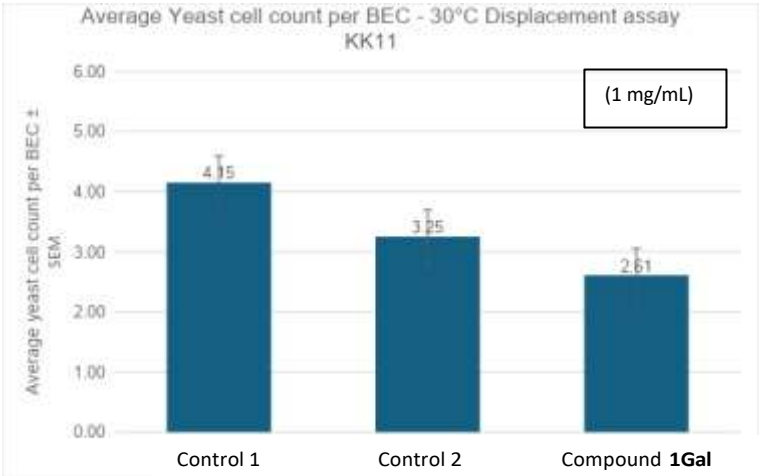

39.5 % reduction against control 1
and 22.7 % reduction against control 2

Figure S-36. *Average yeast cell count per BEC after a displacement assay with compound* ***1Gal****, at a concentration of 1 mg/mL (1.5 mM)*

8. Supplementary References

S1 K. Wojtczak, E. Zahorska, I. J. Murphy, F. Koppel, G. Cooke, A. Titz and J. P. Byrne, *Chem. Commun.*, 2023, **59**, 8384–8387.

S2 H. Martin, M. M. Govern, L. Abbey, A. Gilroy, S. Mullins, S. Howell, K. Kavanagh and T. Velasco-Torrijos, *European Journal of Medicinal Chemistry*, 2018, **160**, 82–93.